COMADEM

International Journal of Condition Monitoring and Diagnostic Engineering Management

Thermal Characterization of Commercial Electric Radiators

Taimoor Asim [a]*, Karina Zala [b], Rakesh Mishra [b], Fiona Conor [c], Scott Conor [c], Naeem Mian [b], Blaise Nsom [d]

[a] *School of Engineering, Robert Gordon University, Aberdeen, UK (AB10 7GJ)*
[b] *School of Computing & Engineering, University of Huddersfield, Huddersfield, UK (HD1 3DH)*
[c] *Trust Electric Heating, Garforth, Leeds, UK (LS25 2JY)*
[d] *Université de Bretagne Occidentale, IUT de Brest, IRDL UMR CNRS 6027, France*

∗ *Corresponding author. Tel.: +44-1244-262457; email: t.asim@rgu.ac.uk*

ABSTRACT

Electric radiators with a storage element are commonly used to provide heating in cold weather. The thermal performance of an electric radiator is dependent on a number of key design features such as the core material, shape of radiator's outer surfaces, gap between the core and the outer surfaces. The effectiveness of an electric radiator can be improved by optimally designing these key features. Researchers around the world have been working to achieve this using a range of different methodologies. In the present study, two commercial electric radiator models have been considered for their thermal characterisation during their individual heating and cooling cycles. This has been carried out in order to evaluate the thermal behaviour of the two models. To achieve this aim, a purpose built test rig has been developed and the thermal testing has been carried out in a controlled environment. A thermal camera has been used to take thermal images of the front surfaces of the two models at every 5 minutes' interval enabling quantification of temperature field. It has been observed that the two electric radiator models considered depict different thermal characteristics. The heat dissipation characteristics of both the models have also been noticed to be different to each other.

Keywords: Electric Radiator; Thermal Camera; Surface Temperature; Radiator Core.

1. Introduction

Electric radiators are commonly used for domestic heating during an undesired fall in environmental temperatures. The main advantages of electric radiators are that it saves living space, working space and is easy to install [1]. Many factors influence the thermal performance of an electric radiator for example, the core material, shape of radiator's outer surfaces, gap between the core and the outer surfaces. Optimising these factors can improve the thermal characteristics of an electric radiator. The literature reports numerous methodologies employed to achieve this [1-5]. Ferrarini et al. [1] used both numerical and experimental methodologies to investigate the thermal behaviour of a standard electric radiant heating panel. In the experimental section of the investigation, the authors have used a controlled environment with temperature sensors and heat flow meters, while a mathematical approach had been developed in the numerical section. The outcomes showed that an efficiency of energy transformation close to one was achieved at steady state. In addition to this, the authors found that the time constant to achieve steady state was quicker than a hydronic system during a transient thermal regime.

Basily and Colver [2] numerically analysed the modelling and the performance of three electric conical heaters. The first conical heater configuration had outer coils, the second had inner coils and the third had both, inner and outer coils. The authors discovered that the configuration that provided the highest efficiency and is the easiest as well as being the cheapest to manufacture, was the conical heater configuration with the outer ring coils. In addition to this, the findings suggested that the performance of the heater could be improved by increasing the coil length and airflow rate, while reducing emissivity of the coil, emissivity of the wall and diameter of the wire. Ning et al. [3] used numerical methodology to develop a classification scheme centered on the thermal response time for the design and control of a radiant system, which describes the dynamic thermal performance more clearly. Freegah et al. [6] studied the effect of different input conditions of heat flux and thermal loading on the performance of a closed-loop solar hot water thermosyphon system. The authors also studied the influence that solar heat flux and thermal loading has on the flow distribution inside the riser pipes of the thermosyphon. Both studies were natural convection investigations using Computational Fluid Dynamics. The authors discovered that there is a predominant influence of the input of heat flux on heat transfer coefficient than thermal loading. They also revealed that there is a considerable influence of solar heat flux, whereas thermal loading has negligible influence on velocity magnitude and static temperature profiles inside the riser pipes [7].

It has been extensively shown that CFD can be used for design and optimisation purposes for a wide variety of applications [8-15], however, the numerically predicted results need to be

validated against well-designed experiments. Hence, in the present study, two commercial electric radiator models have been considered for their thermal characterisation during their individual heating and cooling cycles. This has been carried out in order to evaluate the thermal behaviour of the two models. To achieve this aim, a purpose built test rig has been developed and the thermal testing has been carried out in a controlled environment.
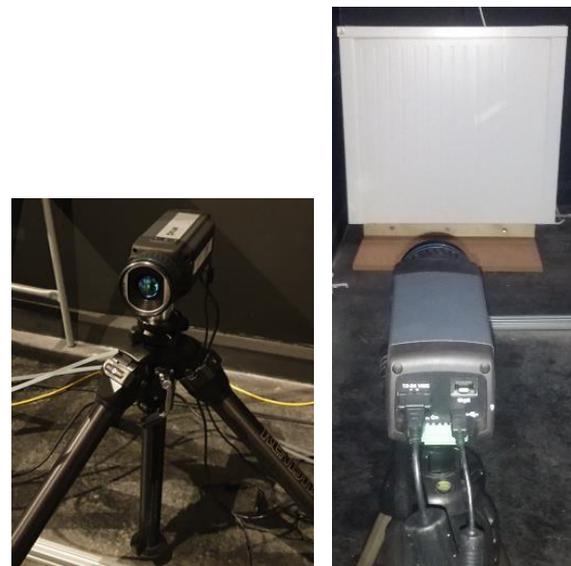
2. Experimental setup

The two electric radiator samples involved in this experimentation are shown in figure 1. Sample-1 has a power rating of 1.2kW, while Sample-2 has a power rating of 1.3kW. The front surface of Sample-1 (figure 1(a)), is a flat plate, while its back surface (figure 1(b)), has depressions in the lower half. There is a gap between the front surface of Sample-1 and its core (figure 1(c)), while there are fins in between the core and the back surface. The front surface of Sample-2 is shown in figure 1(d). The back surface of Sample-2 resembles its front surface. The core (heating element) of the two samples shown in figure 1 are quite different. Sample-1 encompasses a core made of soapstone while Sample-2 encompasses a core made up of clay mixed with aluminium oxide. While the core of Sample-1 is positioned in the centre, the core of Sample-2 is tilted at the top and touches the front surface of the radiator, while the bottom of the core is in between the front and back surfaces of the radiator.

(e)
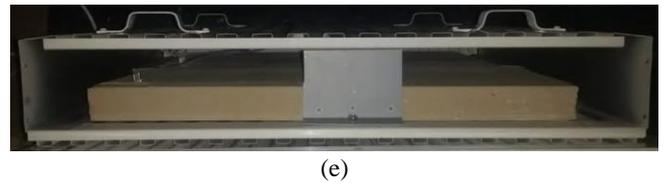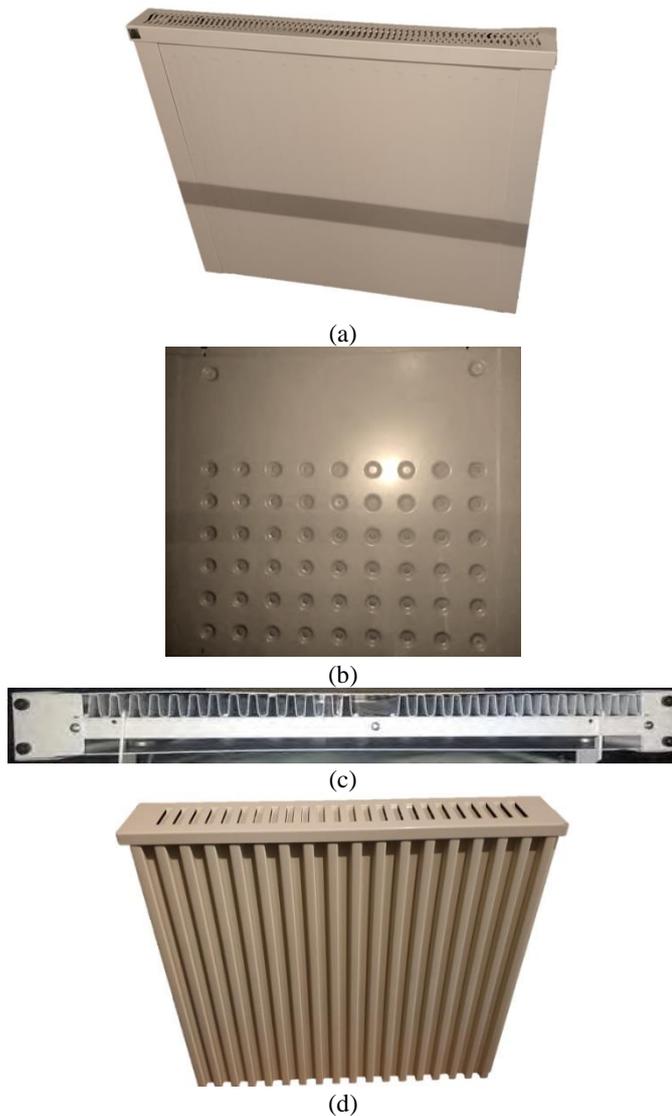
Figure 1. Electric radiators (a) Sample-1 front surface (b) Sample-1 back surface (c) Sample-1 core (d) Sample-2 front surface (e) Sample-2 core

The thermal characterization of the electric radiator samples has been carried out using a thermal camera. The thermal camera used in the present study is FLIR A655sc, and is shown in figure 2(a). The thermal camera used here is based on infrared temperature sensing and is self-calibrating. It is has a resolution of 640 x 480, spectral range of 7.5–14.0μm and accuracy of ±2°C or ±2% of reading [16]. The camera was attached to a tripod to adjust its alignment with respect to the electric radiator. The experimental setup is shown in figure 2(b). The radiator samples have been mounted on a custom-built wooden stand to mimic the effects of back wall. The distance between the camera and the front surface of the samples is 1.9m. Necessary adjustments had been made to avoid reflections from the front surfaces of the samples.

(a)

(b)

(c)

(d)

Figure 2. (a) Thermal camera (b) Setup

The experimental procedure followed during the thermal imaging of the samples is summarized, for both the front and the back surfaces of the sample radiators, as follows:

i.   Mount the radiator sample on the mounting.
ii.   Connect the camera to the PC installed with data analysis software.
iii. Turn the camera on and set the different parameters in the software (like room temperature etc).
iv.   Take a thermal image while the sample radiator is off.
v.   Turn the sample radiator on.
vi.   Take thermal images every 5 minutes till the surface temperature reaches its maximum temperature (heating cycle).
vii. Turn off the radiator.
viii. Take thermal images every 5 minutes till the surface of the radiator is at room temperature (cooling cycle).

3. Results and Discussions

This section presents thermal images that have been captured on the front and back surfaces of the two radiator samples. Both maximum and average temperature values have been recorded. The room temperature at the start of heating cycle was 20℃ for both sample radiators. The front surface temperature values for Sample-1 ranges from 20℃ to 73℃, while it ranges from 20℃ to 130℃ for Sample-2. These are the minimum and maximum temperatures recorded on the front surface of Sample-1 and Sample 2 at 45minutes and at 70minutes, respectively. The maximum, average and minimum temperatures recorded on the front surface at 15minutes of heating for Sample-1 are 40℃, 32℃ and 22℃ respectively, while for Sample-2 these are 59℃, 42℃ and 21℃ respectively.

It is noticed that temperature begins to increase from the top of the radiator for Sample-1 and from the bottom mid-section for Sample-2. The maximum, average and minimum temperatures recorded on the front surface at 30minutes of heating for Sample-1 are 62℃, 45℃ and 25℃ respectively, while for Sample-2 these are 90℃, 61℃ and 23℃ respectively. It can be seen that the heated areas are much more prominent in this timeframe. In case of Sample-1, temperature propagates downwards of the radiator towards the mid-section, while Sample-2 has another high temperature area emerging from the upper mid-section of the radiator. The maximum, average and minimum temperatures recorded on the front surface at 45minutes of heating for Sample-1 are 73℃, 52℃ and 29℃ respectively, while for Sample-2 these are 110℃, 73℃ and 23℃ respectively. Sample-1 has reached its maximum temperature at 45minutes whereas Sample-2 continues to heat up. The maximum, average and minimum temperatures recorded on the front surface at 60minutes of heating Sample-2 are 125℃, 82℃ and 21℃ respectively. It can be noticed that the temperature from the upper mid-section and lower mid-section of the radiator merges to the central region. Moreover, the maximum, average and minimum temperatures recorded on the front surface at 70minutes of heating are 132℃, 86℃ and 25℃ respectively. Prominent high temperature region central of the radiator is observed in this timeframe. The temperature trend of the front surface of Sample-1 radiator is from top to bottom. Thermal distribution between the left and right sides of the sample can be seen to be reasonably uniform.
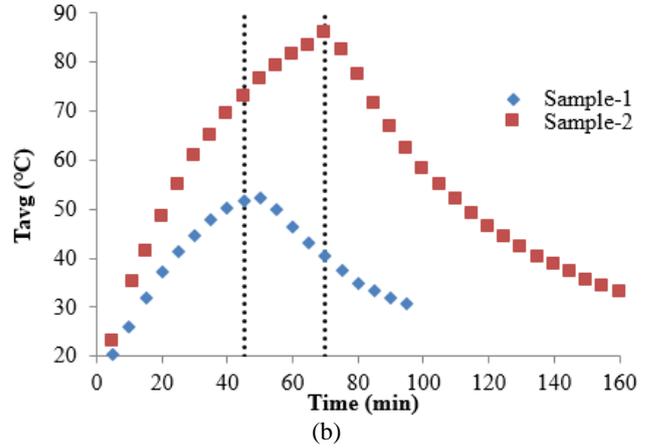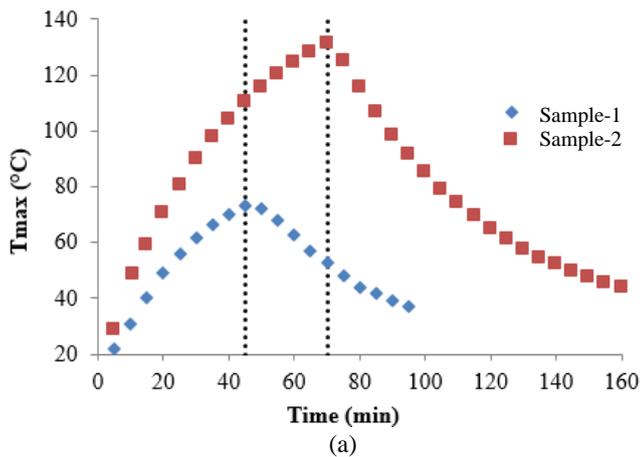
The thermal images reveal that the heating philosophy of Sample-2 is significantly different to Sample-1. In Sample-2, the lower mid-section of the front surface initially heats up and attains the maximum temperature on the surface. The thermal distribution on the front surface of Sample-2 has been observed to be substantially more non-uniform than Sample-1, with localised regions of higher temperature. The higher front surface temperature exhibited in Sample-2 in comparison with that in Sample-1 is a result of the tilted core in Sample-2, which is in contact with the front surface of the radiator, therefore increasing its surface temperature. The thermal efficiency of an electric radiator is associated with its capacity to dissipate heat. As the power rating of both the sample radiators is about the same, higher surface temperature of Sample-2 is indicative of lower heat dissipation in comparison with Sample-1. Hence, Sample-1 is thermally more efficient than Sample-2.
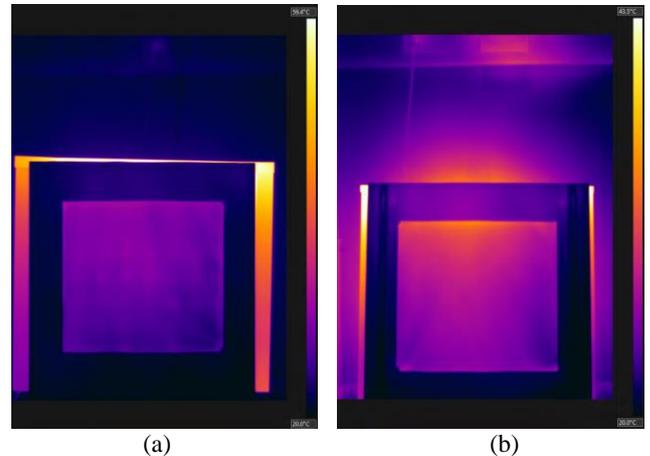
Sample-1   Sample-2

15minutes

30minutes

45minutes

60minutes

70minutes
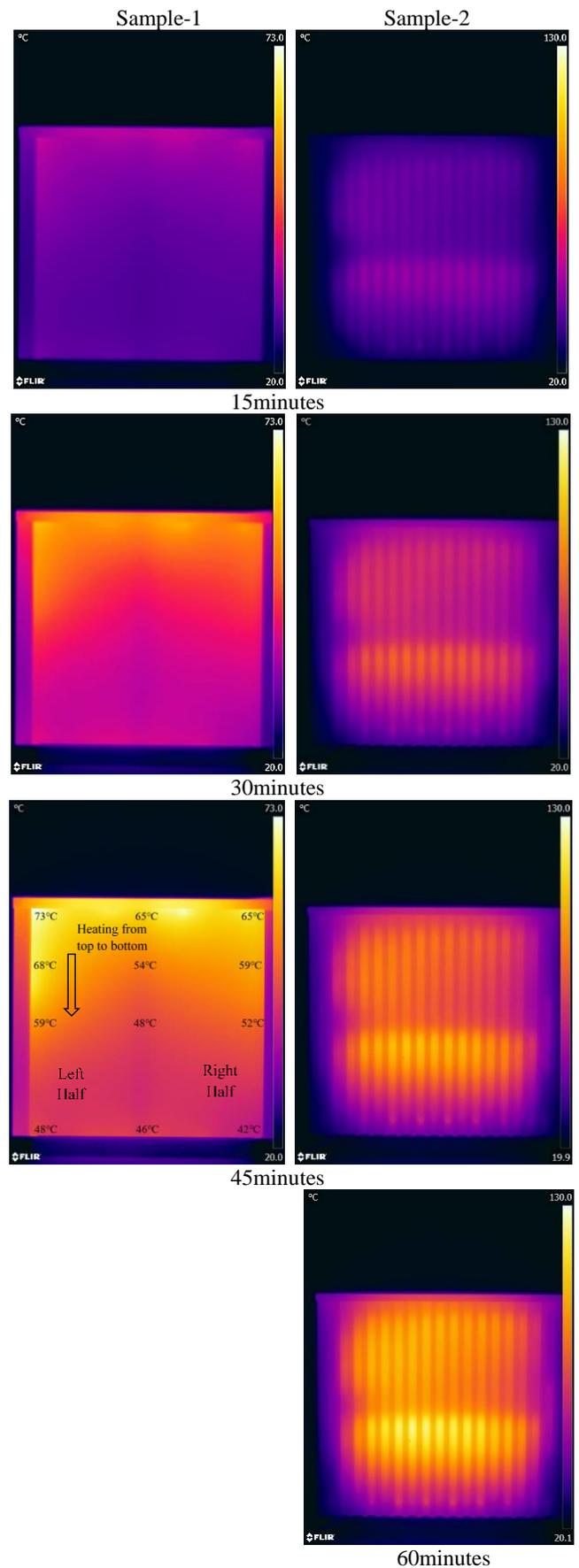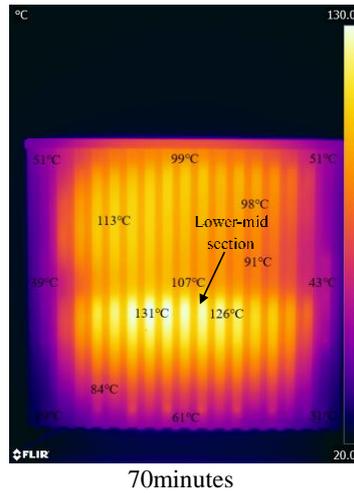
Figure 3. Temperature of the front surface (°C) for (a) Sample-1 and (b) Sample-2

(b)

Figure 4. Variations in (a) maximum and (b) average temperature on the front surfaces of the radiator samples

It can be seen in figure 4 that both maximum and average temperatures on the front surfaces of both radiator samples increase to their maximum values of 73℃ and 52℃ for Sample-1 and 130℃ and 86℃ for Sample-2, at the end of the heating cycle, after which, during the cooling cycle, the values decrease. Both maximum and average front surface temperatures attained by Sample-2 are significantly higher than Sample-1. The primary reason for this behaviour is that mass of the core in Sample-2 is higher. Moreover, the core in Sample-2 is titled towards the top and is in contact with the front surface of the radiator. This further suggests that the heat dissipation in Sample-1 may be predominantly convective, while in Sample-2, it seems to be predominantly radiative. It can be further noticed in figure 4 that both the heating and cooling cycles of Sample-1 are shorter than that of Sample-2, indicating that Sample-1 attains its maximum temperature much sooner than Sample-2. An interesting observation has however revealed that at the maximum temperature, at end of heating cycle, the average temperature on the front surface of Sample-1 is 71% of the maximum surface temperature. This ratio for Sample-2 is 65.3%, which indicates that the thermal distribution in Sample-1 is more uniform than Sample-2. This further suggests that heat dissipation in Sample-1 is more efficient than Sample-2.

Figure 5 depicts the thermal images of the back surfaces of the two radiators, at the end of their respective heating cycles i.e. when the back surfaces are at their maximum temperatures respectively. Figure 5(a) shows Sample-1 while figure 5(b) shows Sample-2. The back surface of Sample-1 reached its maximum temperature in 70minutes. The back surface of Sample-2 reached its maximum temperature in 85minutes. Hence, it is clear that the back surfaces of both the samples took significantly more time to reach their maximum temperatures compared to their respective front surfaces (45minutes for Sample-1 and 70minutes for Sample-2). This increase in peak temperature time for back surfaces is 55% and 21% of their respective front surfaces' peak temperature times. This clearly shows the effects of the depressions on the back surface of Sample-1; increasing convection and heat dissipation.

(a)   (b)

Figure 5. Temperature of the back surface (°C) for (a) Sample-1 and (b) Sample-2

The maximum, average and minimum back surface temperatures, at the end of heating cycles, are 33.1℃, 28.3℃ and 21.3℃ for Sample-1, and 35.3℃, 27.5℃ and 21.1℃ for Sample-2 respectively. Again, the surface temperature of Sample-2 is higher than in Sample-1, indicating more thermal dissipation in Sample-1, making it more thermally efficient than Sample-2.

4. Conclusions

From the work carried out in the present study regarding the thermal characterisation of two electric radiators, namely, Sample-1 and Sample-2, it can be concluded that these two radiators have different heat dissipation characteristics. The results obtained suggest that the possible reason for Sample-1 to

(a)

have lower front and back surface temperatures, is a result of a number of factors such as more thermal dissipation, more convection, non-contacting core, lower core's mass, lower power rating etc. Sample-2 has been shown to dissipate heat predominantly through radiation. Hence, Sample-1 is more suitable for applications where very high surface temperatures are undesirable. Moreover, the non-uniformity in temperature distribution on the front surface of Sample-2 leads towards local regions of higher and lower temperatures. Sample-1, on the other hand, depicts more uniform temperature distribution. It can also be concluded that Sample-1 has shown to be having less thermal gradient during both the heating and cooling cycles in comparison with Sample-2. Sample-2 however, has depicted short time periods of rapid heating and cooling. It can be concluded that for almost the same amount of heat input, the front surface temperature of Sample-1 is lower than Sample-2, making it more suitable for applications where there may be a possibility of direct contact with the radiator surface. More detailed thermal analyses are however required in order to fully characterise Sample-1, which can lead towards its design optimisation.

References

1. Ferrarini, G. Fortuna, S. Bortolin, A. Cadelano, G. (2018). Numerical model and experimental analysis of the thermal behavior of electric radiant heating panels. Applied Sciences. Volume: 8. 206.
2. Bassily, A.M. Colver, G.M. (2004). Modelling and performance analysis of an electric heater. International Journal of Energy Research. Volume: 28. 1269 – 1291.
3. Ning, B. Schiavon, S. Bauman, F.S. (2017). A novel classification scheme for design and control of radiant system based on thermal response time. Energy Build. Volume: 137. 38 – 45.
4. Garavand, A.T. Omid, A. Ahmadi, A. Mohtasebi, S.S. (2017). Intelligent fault diagnosis of cooling radiator based on thermal image processing and artificial intelligence techniques. Modares Mechanical Engineering. Volume: 17. 240 – 250.
5. Carli, M.D., Peron, F., Romagnoni, P.C., Zecchin, R., (2000), Computer simulation of ceiling radiant heating and cooling panels and comfort evaluation in proc. of International Congress Healthy Buildings, Espoo, Finland, 6–10 August, 623 – 628.
6. Freegah, B., Asim, T., Mishra, R., Zala, K., (2015), Numerical Investigations on the Effects of Transient Heat Input and Loading Conditions on the Performance of a Single-phase Closed-loop Thermo-syphon in proc. of 42nd National Conference on Fluid Mechanics and Fluid Power, 14th – 16th December, Surathkal, India.
7. Freegah, B., Asim, T., Mishra, R., (2015), Effect of solar heat flux and thermal loading on the flow distribution within the riser pipes of a closed-loop solar thermo-syphon hot water system in proc. of International Congress on Condition Monitoring and Diagnostic Engineering Management, 1st – 4th December, Buenos Aires, Argentina.
8. Asim, T. Oliveira, A. Charlton, M. and Mishra, R. (2019). Improved Design of a Multi-Stage Continuous-Resistance Trim for minimum Energy Loss in Control Valves. Energy. Volume: 174. 954 – 971.
9. Asim, T. Oliveira, A. Charlton, M. and Mishra, R. (2019). Effects of the Geometrical Features of Flow Paths on the Flow Capacity of a Control Valve Trim. Petroleum science and Engineering. Volume: 172. 124 – 138.
10. Asim, T. Algadhi, A. and Mishra, R. (2018). Effect of Capsule Shape on Hydrodynamic Characteristics and Optimal Design of Hydraulic Capsule Pipelines. Journal of Petroleum Science and Engineering. Volume: 161. 390 – 408.
11. Asim, T. Charlton, M. and Mishra, R. (2017). CFD based Investigations for the Design of Severe Service Control Valves used in Energy Systems. Energy Conversion and Management. Volume: 153. 288 – 303.
12. Asim, T. and Mishra, R. (2017). Large Eddy Simulation based Analysis of Complex Flow Structures within the Volute of a Vaneless Centrifugal Pump. Sadhana. Volume: 42. 505 – 516.
13. Asim, T. and Mishra, R. (2016). Optimal design of hydraulic capsule pipelines transporting spherical capsules. Canadian Journal of Chemical Engineering. Volume: 94. 966 – 979.
14. Asim, T. and Mishra, R. (2016). Computational Fluid Dynamics based Optimal Design of Hydraulic Capsule Pipelines Transporting Cylindrical Capsules. International Journal of Powder Technology. Volume: 295. 180 – 201.
15. Asim, T. Mishra, R. Abushaala, S. and Jain, A. (2016). Development of a Design Methodology for Hydraulic Pipelines Carrying Rectangular Capsules. International Journal of Pressure Vessels and Piping. Volume: 146. 111 – 128.
16. Flir A655sc Datasheet. MathWorks https://www.flir.co.uk/globalassets/imported-assets/document/rnd_011_us.pdf